Roll up nanowire battery from silicon chips

Alexandru Vlad[a,b,1], **Arava Leela Mohana Reddy**[a,1], **Anakha Ajayan**[a], **Neelam Singh**[a], **Jean-François Gohy**[c], **Sorin Melinte**[b], **and Pulickel M. Ajayan**[a,2]

[a]Department of Mechanical Engineering and Materials Science, Rice University, Houston, TX 77005; and [b]Institute of Information and Communication Technologies, Electronics and Applied Mathematics, Electrical Engineering, Université catholique de Louvain, Louvain la Neuve B-1348, Belgium; and [c]Institute of Condensed Matter and Nanosciences, Bio- and Soft Matter, Université catholique de Louvain, Louvain la Neuve B-1348, Belgium

Edited by Jisoon Ihm, Seoul National University, Seoul, Republic of Korea, and approved August 7, 2012 (received for review May 26, 2012)

Here we report an approach to roll out Li-ion battery components from silicon chips by a continuous and repeatable etch-infiltrate-peel cycle. Vertically aligned silicon nanowires etched from recycled silicon wafers are captured in a polymer matrix that operates as Li^+ gel-electrolyte and electrode separator and peeled off to make multiple battery devices out of a single wafer. Porous, electrically interconnected copper nanoshells are conformally deposited around the silicon nanowires to stabilize the electrodes over extended cycles and provide efficient current collection. Using the above developed process we demonstrate an operational full cell 3.4 V lithium-polymer silicon nanowire (LIPOSIL) battery which is mechanically flexible and scalable to large dimensions.

polymer electrolyte | core-shell nanowires | energy storage |
flexible electronics | waste management

Silicon is a promising anode material in lithium batteries due to its high specific capacity and low operation voltage (1). However, the major concern in using Si-based anodes is the huge volume expansion during the lithiation that leads to a fast degradation of the electrode material and a reduced life cycle of the battery with limited use in real life Li-ion applications. The advent of nanotechnology and successful incorporation of nanostructured materials in energy storage devices has further grown an interest in revisiting Si as an active anode material. The enhancement in the electrochemical performance of nanostructured Si anodes provides novel platforms for the ubiquitous presence of Si in Li-ion batteries (2–4). Through nanostructuring, the active Si pulverization was minimized yielding stable capacity retention. However, this was found insufficient to maintain a uniform electrical interface and adequate mechanical contact between the active Si particles and the conductive additives, calling for the development of new binder materials (5–7). Avoiding binders or conductive additives and enabling a direct contact between Si and the current collector is the other way to maintain the electrical conductivity and mechanical integrity of the electrode. This requires special designs of the current collector complying with the ensuing active material deposition. The optimal alternative so far is provided by the use of nanowires, nanotubes, or hierarchical assemblies directly grown, assembled, or bonded onto the current collector (8–12).

Current collectors integrated with Si anodes have been successfully fabricated through chemical or physical vapor deposition methods, room temperature metal assisted chemical etching (MACE), as well as through various top-down methods (8, 9, 12–15). One of the major drawbacks of the respective configurations is the relatively low tap density of the Si nanostructures leading to low mass loading of active material and low volumetric capacities. Moreover, excess of current collector is usually employed in this configuration rendering them less attractive for high-throughput battery manufacturing (16). Low compaction density is intrinsic to nanostructured materials and requires additional processing, including agglomeration and high pressure densification (17). Indeed, these methods do not offer fine adaptation of the composite free space to account for the volume expansion during cycling while not compromising the active component loading. This is of importance primarily when dealing with Si-based anode materials, where the strain and the large volume expansion (up to ≈400%) of the active particles have to be considered upon formation of the fully lithiated $Li_{4.4}Si$ phase (18, 19). Colloidal mask-sustained Si MACE solves this issue and as we show herein, this approach not only allows for large-scale nanowire synthesis through Si waste recycling, it also enables precise tuning of the vertical nanowires morphology (length and diameter) as well as of the nanowire packing density up to nearly the bulk limit. We impregnated the high-aspect ratio (>100) Si nanowire forests with a polymer matrix that acts as a gel-electrolyte and as a physical separator. The polymer-embedded Si nanowire composite can be peeled off the substrate yielding a mechanically robust, freestanding membrane. An electroless growth protocol is developed to wrap the Si nanowires with a thin porous Cu layer. The accordingly obtained $Si_{\text{-core}}$ @ $Cu_{\text{-shell}}$ nanowires display enhanced electrochemical performances due to improved current collection efficiency and Si encapsulation. A functional 3.4 V LIPOSIL (lithium-polymer silicon nanowire) battery is demonstrated by laminating a $LiCoO_2$ cathode layer on top of the Si nanowire—polymer composite.

Results and Discussion

Design and Fabrication of LIPOSIL Composites. For the nanowire synthesis, we employed a continuous Si MACE (20, 21) with various seeding layers (Fig. 1). Colloidal nanosphere lithography was used to structure the catalyst layer (see Fig. 1 *A–C* and *Materials and Methods*). The diameter and spacing of the nanowires can be precisely controlled by the size of the colloidal particles and subsequent processing conditions, while their length is adjusted by the etching time (see *SI Text*, Fig. S1). Depending on the catalyst type, it is possible to etch silicon at rates higher than 1 μm/min (see *SI Text*, Fig. S2). Controlling the diameter, the spacing and the height of the nanowires, facilitates smart tuning of the morphology that directly impacts (i) the electrode mass loading, (ii) the free volume conforming to the Si volume expansion whilst cycling, and (iii) the impregnating volume of polymer, which is responsible for electrolyte uptake and attainment of the conducting gel electrolyte. Adequate balancing of these criteria is the key to optimal electrochemical performances of the LIPOSIL anode composite. An excess active material loading by using large diameter nanowires will preclude the free space for volume expansion accommodation and appropriate electrolyte amount uptake, while the reverse will result in low active material loading into electrodes. Note that ~10% free space can be achieved if the

---

Author contributions: A.V., A.L.M.R., and P.M.A. designed research; A.V., A.L.M.R., A.A., and N.S. performed research; A.V. and A.L.M.R. contributed new reagents/analytic tools; A.V., A.L.M.R., J.-F.G., S.M., and P.M.A. analyzed data; and A.V. and A.L.M.R. wrote the paper.

The authors declare no conflict of interest.

This article is a PNAS Direct Submission.

[1] A.V. and A.L.M.R. contributed equally to this work.

[2] To whom correspondence should be addressed. E-mail: ajayan@rice.edu.

This article contains supporting information online at www.pnas.org/lookup/suppl/doi:10.1073/pnas.1208638109/-/DCSupplemental.

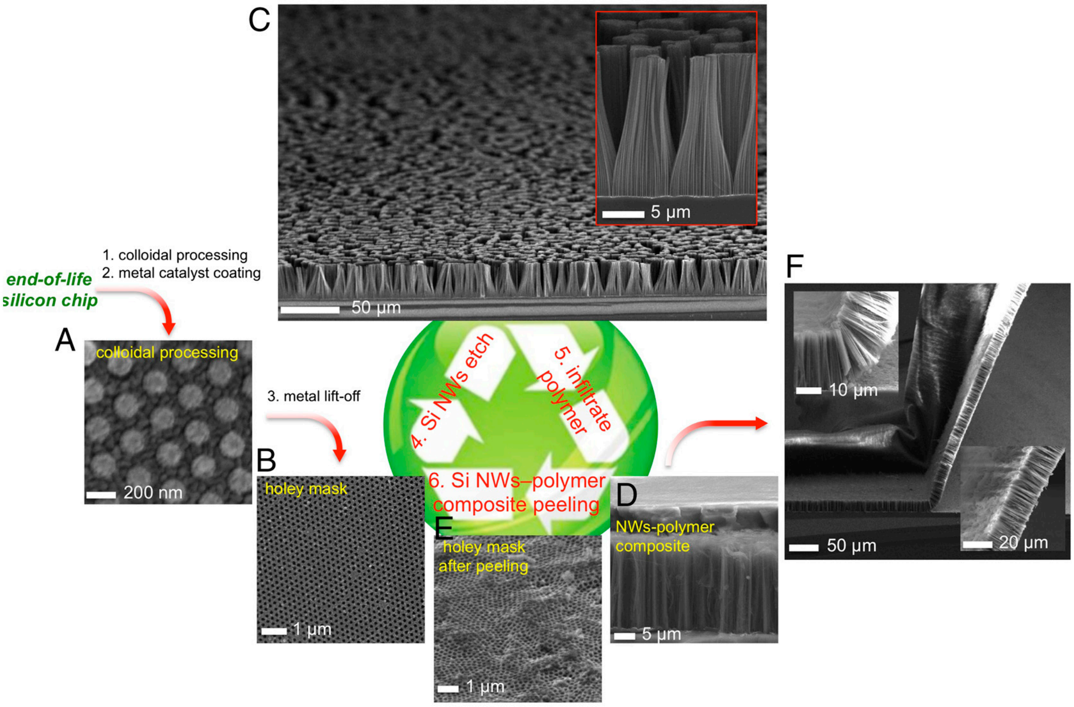

Fig. 1. *A second life for silicon: Si chip towards the Li-battery recycling wheel.* Schematic of the Si-polymer composite fabrication: (*A*) colloidal polystyrene particles are self-assembled and processed on a Si chip to realize the (*B*) holey Au mask used to fabricate the (*C*) Si nanowires through MACE. Uniform diameter and length nanowires are obtained over large areas (*Inset*). (*D*) After the polymer/electrolyte infiltration, the composite is mechanically peeled to obtain the (*F*) self-supported Si nanowire-polymer composite. The fabricated composite membrane is highly flexible and can be bent with curvature radii less than 15 µm (*Inset*, see also Fig. 2*C*). (*E*) The holey catalyst mask remains intact after the peeling step and it is re-used for the fabrication of further Si nanowire-polymer composite membranes until the physical exhaustion of the Si chip.

colloidal particles are not reduced in size. A Si nanowire forest consisting of $\sim$25 µm long nanowires with a diameter of $\sim$150 nm (with 260 nm lattice spacing defined by the colloid packing), has a free space approximately 70% of the total volume, corresponding to a mass loading of 1.75 mg/cm^2. Experimentally we found a similar value of $\sim$2 mg/cm^2 with the small variation being attributed to the processing variations and measurements errors. Higher mass loading, without compromising the free volume, can be achieved via longer nanowires by simply increasing the etching time (see *SI Text*, Fig. S2).

Direct implementation as battery anodes of the substrate-supported Si nanowires is not desirable since the remaining bulk Si is prone to pulverization and the physical link to nanowires would be rapidly lost. By embedding the nanowires into a polymer host, we obtain a composite that could be readily peeled off in the form of a flexible and robust freestanding membrane (Figs. 1 and 2). In the composite membrane, the nanowires maintain their alignment and have one end exposed for the electrical connection. By adding excess polymer during the infiltration, a separator layer is formed on top that makes an integrated unit of separator—anode (Fig. 1*D*). From a typical battery composition picture, our anode can be considered as binder-free and the polymer of choice must present the following characteristics: (i) mechanical stability in the composite form, (ii) electrochemical stability in a wide potential window, and (iii) good gel-polymer properties, i.e. large electrolyte uptake and high ionic conductivities. To comply with these characteristics we have selected a poly(vinylidene fluroride-*random*-hexafluoropropylene) copolymer because of its excellent mechanical characteristics and electrolyte swelling properties. Addition of 5–10% silica nanoparticles was found to enhance the electrochemical performance of the LIPOSIL composite. The polymer infiltration was performed with a 5% wt. acetone solution. Conformal coating of the Si nanowires failed when simply adding and drying an excess polymer solution. Indeed, a continuous polymer film formed on top of the substrate without infiltrating the nanowires (see *SI Text*, Fig. S3) presumably due to a fast evaporation rate of the solvent within the high surface area Si nanowire forest. In order to conformally entrap the Si nanowires, we proceeded with successive polymer coatings, using a modified paint battery technique (22), followed by drying steps until a continuous polymer film was detected on the surface of the sample (Fig. 2 *A* and *B*). The fully impregnated LIPOSIL composite was then peeled off from the substrate and the freestanding membrane was robust enough for subsequent processing through rolling, wrapping, bending and lamination (Figs. 1 and 2).

Silicon Chip Recycling Scheme. Since the colloidal processing may be regarded as an extra-processing step with additional costs for the battery fabrication, we have implemented a multi-loop MACE—polymer infusing—composite peeling protocol. In this respect, we succeeded in realizing up to four LIPOSIL composite anode membranes out of a single Si chip, while fabricating the MACE catalyst mask only once (schematic of the recycling is depicted in Fig. 1). The key to implement the multi-loop protocol is the preservation of the MACE mask during the processing (Fig. 1*E*). Even after several |silicon MACE|—|polymer infuse|—|LIPOSIL composite peeling| fabrication steps, the mask preserves its integrity by producing high quality nanowire arrays (Fig. 2 *C–E*). The major limiting factor of the present fabrication protocol is the initial thickness of the Si chip. For example, the MACE mask could be further used after delaminating four composite membranes (Fig. 2*C*) out of a 330 µm thick Si chip. However, the fragility of the remained $\sim$150 µm thick Si wafer rendered the next processing step difficult (for the illustration purpose, the chosen Si nanowire height was $\sim$40 µm). By using iteratively the MACE protocol, with four of those cycling loops, more than half of the Si chip was transformed into a multifunctional nanostructured composite. Considering that the modern microelectronics industry uses approximately 35.000t of Si each year (23), and this amount is susceptible to become in the near future a hardly recyclable waste—biodegradability or semiconducting industry re-integration can be excluded, our scheme could provide an alternative for a better waste management of this resource. Though we target here their use as Li battery anodes, the respective composite membranes could find use as photovoltaic or photo-electrochemical energy harvesting

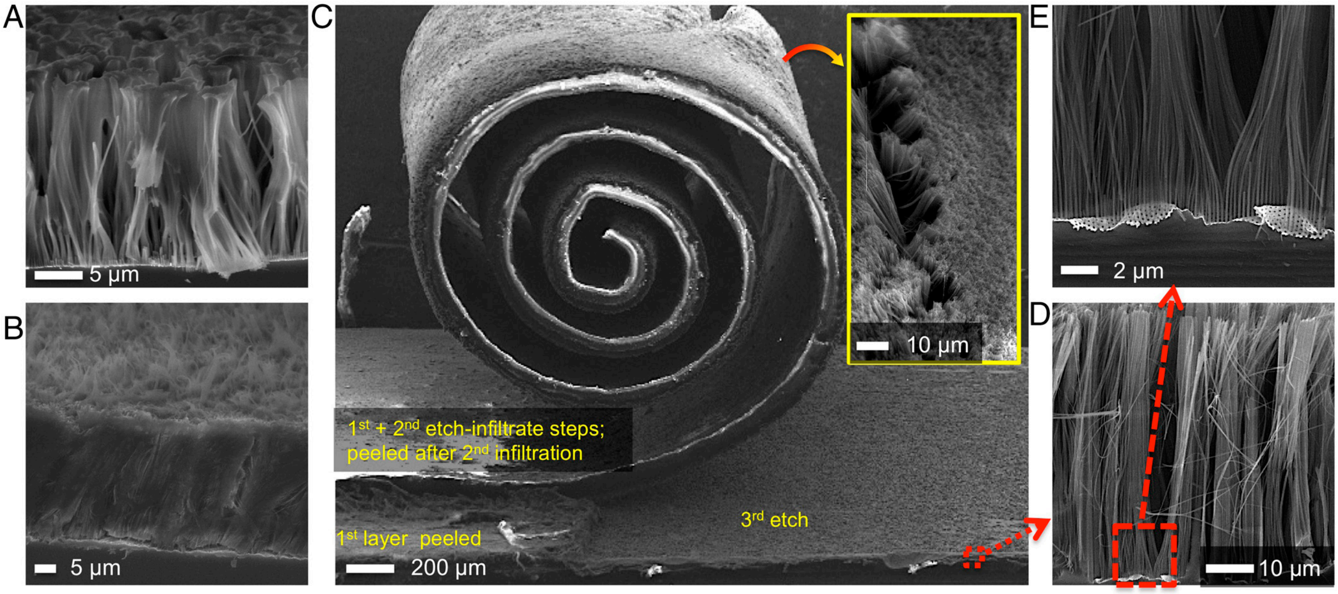

Fig. 2. *Polymer infiltration and multi-peeling protocol.* (*A*) Partial infiltration showing the conformal coating of single and bunches of nanowires. (*B*) Fully infiltrated Si nanowires. (*C*) Exemplification of the multi-loop etch-infiltrate-peel protocol. Three consecutive etch-infiltrate-peeling processing loops have been performed on the same Si chip and using the same MACE mask. (*Inset*) Back-side of the peeled membranes, showing the exposed nanowires for current collector contact. (*D*, *E*) Even after several etch-infiltrate-peel steps, the MACE mask maintains its integrity and continues to provide high-quality Si nanowires arrays.

components, antireflective, or hydrophobic coatings. More generally, the proposed fabrication approach might enable a fast and reliable synthesis and device integration of bulk quantities of hybrid Si nanowires with controllable characteristics (24–26).

Electrochemical Characterization. The as-prepared polymer-entrapped Si nanowire membranes display competent electrochemical performance when cycled in half-cell configuration. Prominently, the addition of inorganic fillers (5–10% wt. of fumed silica) to the PVDF-HFP matrix enhances cycling performance owing to higher electrolyte uptake and ionic conductivity (27). In the cyclic voltammogram of the pristine nanowires (Fig. 3), a characteristic peak at ~0.5 V is suggestive of alloy formation of Li with Si and a peak at ~0.7 V is indicative of de-alloying process. The peak at ~1.5 V in the first cycle is related to electrolyte decomposition and solid-electrolyte interface (SEI) formation and becomes less pronounced in subsequent cycling. An initial discharge capacity of ~3500 mAh/g is achieved at a C/20 cycling rate (C-rate defined as 1C = 1 h to discharge). The capacity loss in the first cycle (~1000 mAh/g) is mainly attributed to the structural imperfections and accidental loss of the electrical contact between the high aspect ratio Si nanowires and the thin-film current collector as well as to SEI formation. The mechanical peeling process was found to strongly influence the electrochemical performance. The process involves a "manhandled" laboratory stainless-steel blade (tip curvature radius of aprox. 10 µm) to crack the base of nanowires and peel-off the LIPOSIL composite. This leads to partial damaging of the nanowires, especially at the peeled base (notified by the presence of dusty residuals on blade, substrate, and LIPOSIL membrane). Clearly, the damaged nanowires will be first to fail upon

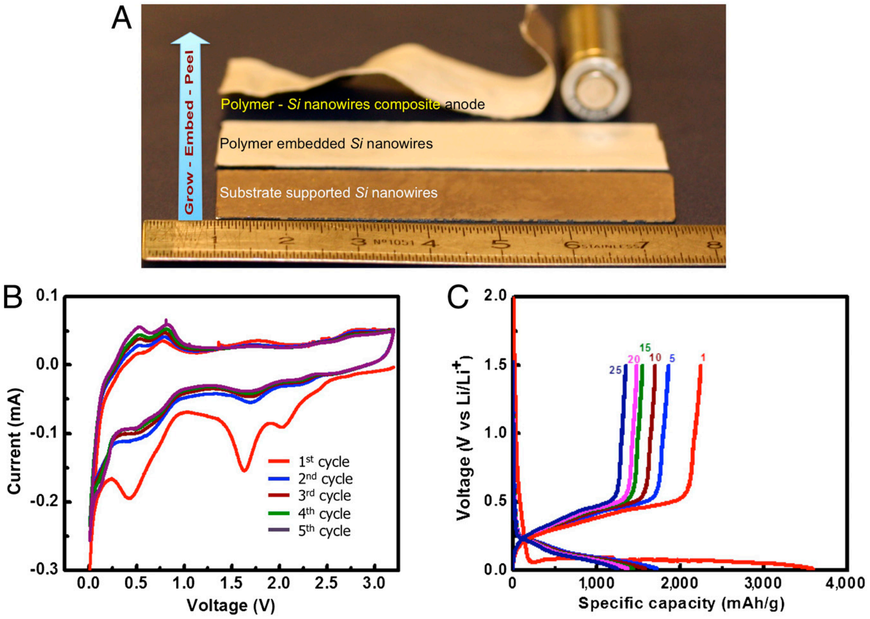

Fig. 3. *Electrochemical performance of Si nanowire-polymer composite.* (*A*) Ensemble view of the large-scale LIPOSIL processing flow. Commercial battery-scale fabrication is achieved. (*B*) Cyclic voltammetry curves of the polymer wrapped silicon nanowires anodes between 3.2 V and 0.02 V by soaking the polymer in 1M solution of $LiPF_6$ in 1:1 (v/v) mixture of Ethylene Carbonate (EC) and Dimethyl Carbonate (DMC). (*C*) Galvanostatic discharge/charge profiles of the Si—polymer composite cycled at a rate of C/20 between 1.5 V and 0.02 V *vs* Li/Li^+.

cycling. Another factor strongly influencing the cycling behavior is the concomitant delamination of the residual silicon film. The devices where this effect was pronounced displayed severe capacity degradation due to the pulverization of the silicon film upon cycling and subsequent contact loss with the silicon nanowires contained within the LIPOSIL membrane. Unavoidably, most of the peeled membranes contained small areas where the residual silicon film was present. Further optimization could imply the use of automatic, high-precision cutting techniques such as microtome or laser cutting. Nevertheless, the LIPOSIL composite was found to retain a cycling capacity of >1000 mAh/g after 30 cycles while being further improved through copper coating. After cycling, the robustness of LIPOSIL membranes is preserved as no clear signs of degradation could be detected.

Conformal Copper Coating of Silicon Nanowires. Given the specific configuration of the LIPOSIL composite—high aspect ratio nanostructures wired to the planar current collector only at the base—the rather moderate cycling performances and rate capabilities are not surprising. Even if this configuration allows for a rapid radial diffusion of Li$^+$ and a facile stress accommodation, the current collection efficiency is low. This is also valid for highly doped Si nanowires, where the loss in electrical conductivity of the nanowires is observed upon initial cycling (2). Moreover, the Si surface is directly exposed to electrolyte resulting in an excessive SEI layer formation that lowers both the capacity and the Coulombic efficiency. To enhance the electrical conductivity and protect the Si nanowires surface from the direct electrolyte exposure, we have grown a thin Cu layer on the surface of the nanowires (Fig. 4*A*). The metal layer is conformal and uniform over the entire nanowire length (Fig. 4*B*). By properly adjusting the growth time, it can be tailored into a porous structure in the form of interconnected Cu grains decorating the surface of the Si nanowires. This originates from the electroless reduction of Cu^{2+} ions at the Si surface (see *SI Text*, Fig. S4, and *Materials and Methods*). During the initial stages of deposition, the Si nanowires are decorated with a discontinuous layer of Cu nanoparticles evolving into a continuous porous network, while extended deposition produces a thick and continuous Cu matrix embedding the Si nanowires (Fig. S4).

Metallic Cu is not a Li-ion blocking material; the diffusion of Li ions is also possible through a continuous Cu-shell (with a diffusion coefficient of the order of $\sim 10^{-6}$ cm^2 s^{-1}). It has been already shown that Cu-coated Si anodes display improved electrochemical performances and Cu layer thicknesses of up to 100 nm were found to minimally impact the rate performance (28). Here, growing a continuous Cu layer reduced the free-volume for the polymer uptake (Fig. S4) and rendered the composite membranes brittle and fragile. Of primordial importance is the ability to control the growth of thin conformal metal layers on high-aspect ratio silicon nanowires. While physical vapor deposition methods are suitable for morphology and thickness control (29, 30), complex morphologies cannot be coated conformally due to the directionality of these methods. Chemical methods are more suitable. However, minor attention has been attributed to the fine morphology of the copper deposits typically resulting in rough agglomerates at the silicon surface and has been primarily applied to powder processing technology (31–33). We optimized the Cu deposition to allow precise control over the copper thickness and morphology within the dense silicon nanowire forest (Fig. S4). The porous and interconnected configuration of the Cu shell can be regarded as a metallic grid wrapped around the nanowires and electrically wired to the current collector (Fig. 4*C*). This configuration is expected to provide better electrochemical stability and cycling rate performance to the LIPOSIL composite. The metallic nature of the Cu shell increases the electrical conductivity of the nanowires and improves the charge collection efficiency (34–36). At the same time, the porosity of the shell structure allows fast Li$^+$ diffusion towards the surface of Si and helps maintaining structural integrity of the nanowires due to the ductile nature of copper. As compared to the reverse configuration, i.e. the $\mathrm{Cu}_{\text{-core}}$ @ $\mathrm{Si}_{\text{-shell}}$, the present $\mathrm{Si}_{\text{-core}}$ @ $\mathrm{Cu}_{\text{-shell}}$ design is expected to provide similar performance in terms of charge collection efficiency. However, wrapping the Si core rather than using a Si shell, not only improves the mechanical stability upon volume expansion, it also drastically limits the amount of Si in

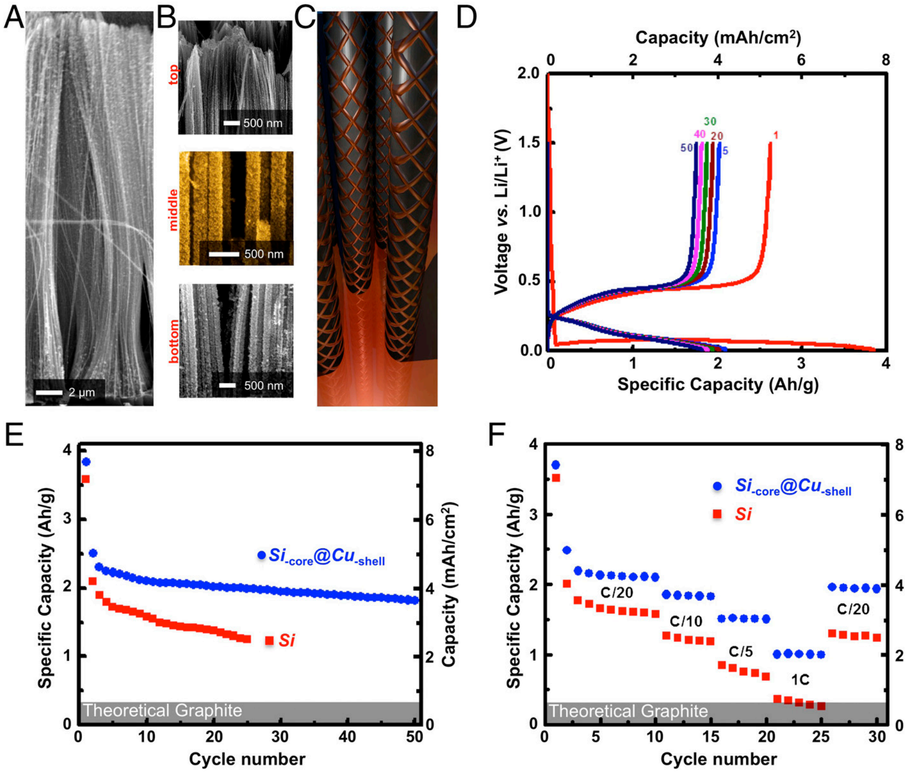

Fig. 4. *Improving the electrochemical performance of composite anodes through conformal copper coating.* (*A*) Conformal Cu coating of high aspect ratio Si nanowires with coaxial morphology through an electroless deposition protocol. (*B*) Snapshots at different height positions evidencing the uniform Cu coating along the Si nanowires. (*C*) Schematic representation of the Cu-wrapped Si nanowires. The Cu shell has a porous, electrically interconnected structure to allow for a faster Li$^+$ insertion, volume expansion accommodation and efficient current collection. (*D*) Discharge/charge profiles for the $\mathrm{Si}_{\text{-core}}$ @ $\mathrm{Cu}_{\text{-shell}}$ composite anodes cycled between 1.5 and 0.02 V. (*E*) Capacity retention at a cycling rate of C/20 of the Si and $\mathrm{Si}_{\text{-core}}$ @ $\mathrm{Cu}_{\text{-shell}}$ polymer electrolyte composite anodes. (*F*) Rate capability of the Si and $\mathrm{Si}_{\text{-core}}$ @ $\mathrm{Cu}_{\text{-shell}}$ polymer electrolyte composite anodes. The theoretical capacity of graphite is highlighted for comparison.

direct contact with the electrolyte and thus, helps in building a stable passive SEI layer.

As expected, the LIPOSIL composite with Si$_{\text{-core}}$ @ Cu$_{\text{-shell}}$ nanowires displays improved performance compared to the LIPOSIL composite with pristine Si nanowires (Fig. 4*D*). The first discharge capacity of ~3900 mAh/g is higher than for pristine Si nanowires (3550 mAh/g) and the composite with Cu$_{\text{-shell}}$ nanowires is able to sustain a capacity of ~2000 mAh/g over extended cycling with little capacity decay. This is equivalent to 4 mAh/cm^2 or 1600 mAh/cm^3, competing with commercial anode formulations with capacities in the range of 3–5 mAh/cm^2 (37). While the first cycle capacity loss is presumably due to structural imperfections and contact failure with the thin-film current collector as already discussed, the pristine composite with bare Si nanowires shows a more marked degradation upon cycling. The improvement clearly arises from the conductivity enhancement of the Cu-coated nanowires. Since the nanowires exhibit high aspect ratio and are connected only at one end, a voltage polarization builds up along the nanowires during the current injection/collection. Therefore, the Si nanowires are expected to be fully lithiated in the regions close to the current collector whereas the Si at the opposite end of the nanowires should reach a lower lithiation level. Furthermore, since the Si conductivity degrades rapidly upon lithiation, subsequent cycling will intensify the effect for the bare Si nanowires anodes by lowering further the amount of electrochemically accessible Si and hence, inducing a rapid capacity decay. The Cu coating rules out the conductivity limitations and enables lithiation of the entire Si mass not only at the first discharge, but also during the subsequent cycling. Further, good electrical contact between the Si electrode and the Cu current collector was evidenced by performing galvanostatic charge/discharge measurements on Si$_{\text{-core}}$ @ Cu$_{\text{-shell}}$ LIPOSIL composite films at different current rates. Fig. 4*E* shows the detailed high rate cycling results for the Si$_{\text{-core}}$ @ Cu$_{\text{-shell}}$ LIPOSIL and bare LIPOSIL composite films. Stable nominal capacity was attained at a C-rate of C/20. Subsequent cycling was conducted at higher current rates as shown in Fig. 4*E*. For Si$_{\text{-core}}$ @ Cu$_{\text{-shell}}$ nanowires, the LIPOSIL composite delivers much higher capacity with the increase in the cycling rate than the bare LIPOSIL composite. For example, at 1C rate, the Si$_{\text{-core}}$ @ Cu$_{\text{-shell}}$—LIPOSIL delivers a reversible capacity of ~1000 mAh/g compared to only ~350 mAh/g for the uncoated nanowires. Also, Si$_{\text{-core}}$ @ Cu$_{\text{-shell}}$—LIPOSIL retains its nominal capacity when it is operated back at lower current rates. The results of high rate electrochemical studies prove that the Si$_{\text{-core}}$ @ Cu$_{\text{-shell}}$—LIPOSIL electrode-electrolyte composite could be used as a good high rate electrode material. The direct contact between the Si electrode and the porous Cu current collector leads to a reduced electronic resistance, hence resulting in improved rate capability of the electrode.

We have also carried out a preliminary study to test the Si$_{\text{-core}}$ @ Cu$_{\text{-shell}}$—LIPOSIL composite assembly in a complete Li-ion cell configuration by casting LiCoO$_2$ cathode slurry on top. Since the LIPOSIL composite makes a continuous PvDF-HFP polymeric phase, defining both the anode and the electrical separator (Figs. 1*D* and 2*B*), it allows the deposition of subsequent layers having similar composition. For instance, we have casted a LiCoO$_2$ cathode layer on top the LIPOSIL composite and built a flexible Li-ion battery with composite Si-nanowire anodes (mass loading of the Si nanowire anode and the LiCoO$_2$ cathode was 1 to 25 weight ratio). When galvanostatically cycled between 2.8 and 4 V (Fig. 5), the cell delivered an initial capacity of 155 mAh/g at a current rate of C/20 (with respect to the cathode mass). The battery operates at an average voltage of 3.4 V (Fig. 5*B*) with little capacity decay for the first 30 cycles. The first cycle Coulombic efficiency is ~80% and following cycles around 90% (Fig. 5*C*).

To summarize, LIPOSIL—the lithium-polymer silicon nanowire battery concept is demonstrated. Precise composition and design of the Si nanowire-based battery anodes are achieved through controlled metal assisted chemical etching of silicon. This enables tailoring of active component loading and free-volume in the electrode for efficient polymer-electrolyte uptake and battery functioning. A straightforward electroless copper coating yields high-aspect ratio Si$_{\text{-core}}$ @ Cu$_{\text{-shell}}$ nanowires. The conformal Cu-wrapped Si nanowires show improved capacity retention and rate capabilities as compared to pristine nanowires when integrated into LIPOSIL architecture. The present work provides a solution for electronics waste management by allowing a second life for Si via LIPOSIL anodes recycled from end-of-life Si chips. As demonstrated, the concept is feasible at the laboratory scale and could become economically viable at larger scale.

Materials and Methods

Silicon chips (orientation 100, *p*-type 15 Ω/cm) have been used without any special surface treatment. A short plasma oxygen exposure was performed in order to render their surface hydrophilic for the colloidal assembly.

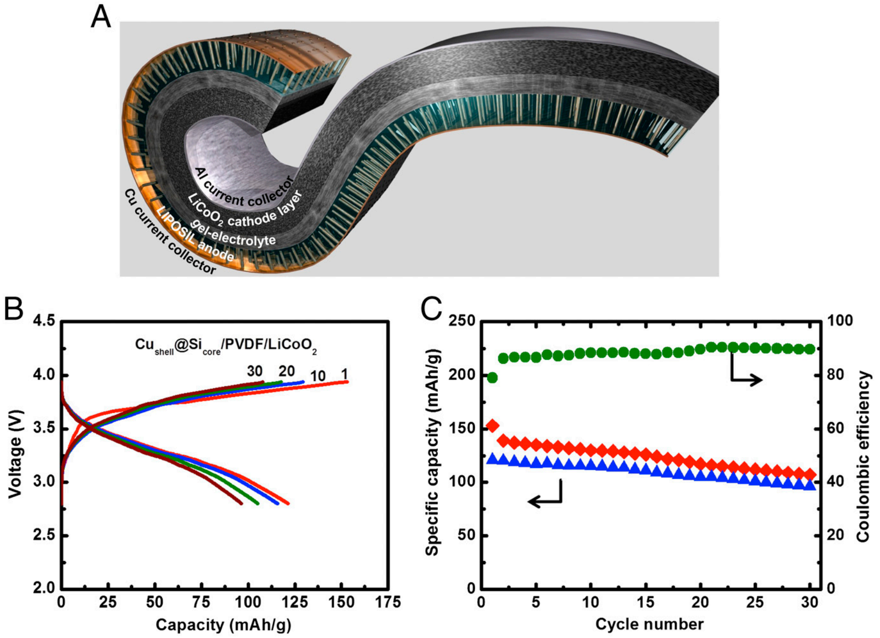

Fig. 5. *3.4 V LIPOSIL with composite nanowire anodes.* (*A*) Schematic view of the rolled LIPOSIL full cell architecture. (*B*) Charge-discharge profiles for the LIPOSIL battery with a spray coated LiCoO$_2$ cathode layer onto the assembled Si nanowires-polymer composite. (*C*) Cycling performance and Coulombic efficiency of the LIPOSIL full cell, cycled between 4 and 2.8 V at a current rate of C/20 rate (capacity is given with respect to weight of LiCoO$_2$).

Polystyrene colloidal particles (260 nm nominal diameter, Microparticles Gmbh) have been used as received. The colloidal self-assembly lithography was done by carefully spreading a diluted colloidal suspension (1∶5 v∶v in ethanol with 0.5% wt. styrene and H_2SO_4 additives) at the water-air interface. After the compaction of the colloidal monolayer through addition of TX100 surfactant, the film was transferred on the pre-treated Si chips and let dry in air. Oxygen reactive ion etching was used to reduce the colloid size, while preserving the hexagonal packing (25 W RF power, 15 mTorr, 50 sccm O_2). A 30 nm thick Au film was subsequently deposited by physical vapor deposition. Adhesive tape was employed to perform the metal lift-off. The MACE was performed in an aqueous solution containing 4.8M HF and 0.2M H_2O_2 in ambient conditions under continuous agitation. The length of the nanowires was set by the reaction time (etch rate ∼500 nm/min). The reaction was quenched by immersing the sample into $CH_3OH:H_2O$ (1∶1 v∶v). The samples were let dry in air.

The PvDF-HFP (Kynar Flex 3801, Arkema Inc.) was used as received. The polymer was dissolved in acetone (5% wt.) with the addition of various amount of fumed silica (5–10% wt. with respect to the PvDF-HFP amount). The Si nanowire infiltration was performed in a layer-by-layer approach. Briefly, a limited amount of PvDF-HFP solution was spread on the surface of samples using a painting brush (22). Once the solution infiltrated the nanowire forest, the excess solution was removed using the brush. This avoids having a thick polymer film formed at the top of the nanowires. This step was repeated until no more distinctive aspect changes could be detected upon addition of the polymer solution. At this point, the nanowire arrays were considered as being fully infiltrated. Subsequent addition resulted in the formation of a polymer film on top of the nanowires used as battery separator. The composite was let dry in air. The white appearance of the top part of the composite signified complete solvent evaporation as well as the fact that the polymer displays micro-porous structure. The nanowire composite peeling was performed manually using a laboratory stainless-steel blade. To realize the current collector, the backside of the membrane was coated first with 25-nm Ni followed by 500-nm Cu using physical vapor deposition.

Conformal Cu coating was realized using an electroless plating protocol. The pristine Si nanowire samples were immersed in an aqueous solution containing 0.04M $CuSO_4$, 0.08M EDTA, and 0.09M CH_2O at 65 °C. The pH of the solution was adjusted to 12 using a TMAH solution. To obtain the porous Cu shell, a reaction time of 30–60 min was applied. The reaction was quenched by immersing the samples in methanol. The samples were rinsed with methanol and water and let dry in air. The samples were exposed to a rapid thermal annealing step (350 °C for 1 min under continuous Ar flow). The polymer infiltration and composite peeling was performed following the same protocol as for the non-coated nanowires.

The electrochemical performance of the LIPOSIL composite films was assessed by galvanostatic charge-discharge experiments. For half cell measurements, test cells were assembled in Swagelok-type cells inside an Ar-filled glove box using the LIPOSIL electrode/separator films as the working and lithium metal foils as the counter/reference electrodes. For full cell measurements, the cathode was made of $LiCoO_2$ (SIGMA ALDRICH), carbon black and PVDF binder in the weight ratio of 85∶10∶5. The slurry was prepared by stirring the above mixture of $LiCoO_2$, carbon black and PVDF in NMP thoroughly, followed by casting onto the above-prepared LIPOSIL composite films. After vacuum drying the resultant structures, an Al thin film is coated by sputtering to serve as a cathode current collector. Both half and full cells were soaked in 1 M solution of $LiPF_6$ in 1∶1 (v/v) mixture of ethylene carbonate (EC) and dimethyl carbonate (DMC) for 1 h prior to the electrochemical studies. Cyclic voltammetry measurements were performed with an AUTOLAB PGSTAT 302N and all galvanostatic charge-discharge measurements were conducted using an ARBIN BT 2000 Battery Analyzer.

ACKNOWLEDGMENTS. A.L.M.R. and P.M.A. acknowledge the financial support from Army Research Office. A.V. and S.M. acknowledge F.S.R. and F.R.S.-FNRS for financial support. S.M. and J.F.G. acknowledge financial support from TINTIN project—ARC, Communauté Française de Belgique, and Région Wallonne (Programme ERABLE).

1. Huggins RA (1999) Lithium alloy negative electrodes. *J Power Sources* 81:13–19.
2. Chan CK, et al. (2008) High-performance lithium battery anodes using silicon nanowires. *Nat Nanotechnol* 3:31–35.
3. Choi N-S, Yao Y, Cui Y, Cho J (2011) One dimensional Si/Sn—Based nanowires and nanotubes for lithium-ion energy storage materials. *J Mater Chem* 21:9825–9840.
4. Szczech JR, Jin S (2011) Nanostructured silicon for high capacity lithium battery anodes. *Energy Environ Sci* 4:56–72.
5. Bridel JS, Azais T, Morcrette M, Tarascon J-M, Larcher D (2010) Key parameters governing the reversibility of Si/Carbon/CMC electrodes for Li-ion batteries. *Chem Mater* 22:1229–1241.
6. Kovalenko I, et al. (2011) A major constituent of brown algae for use in high-capacity Li-ion batteries. *Science* 334:75–79.
7. Liu G, et al. (2011) Polymers with tailored electronic structure for high capacity lithium battery electrodes. *Adv Mater* 23:4679–4683.
8. Chen X, et al. (2010) Virus-enabled silicon anode for lithium-ion batteries. *ACS Nano* 4:5366–5372.
9. Song T, et al. (2010) Arrays of sealed silicon nanotubes as anodes for lithium ion batteries. *Nano Lett* 10:1710–1716.
10. Hwang TH, Lee YM, Kong B-S, Seo J-S, Choi JW (2012) Electrospun core-shell fibers for robust silicon nanoparticle-based lithium ion battery anodes. *Nano Lett* 12:802–807.
11. Wu H, et al. (2012) Stable cycling of double-walled silicon nanotube battery anodes through solid-electrolyte interphase control. *Nat Nanotechnol* 7:310–315.
12. Evanoff K, et al. (2012) Towards ultrathick battery electrodes: Aligned carbon nanotube-enabled architecture. *Adv Mater* 24:533–537.
13. Krishnan R, Lu T-M, Koraktar N (2011) Functionally strain-graded nanoscoops for high power Li-ion battery anodes. *Nano Lett* 11:377–384.
14. Huang R, Fan X, Shen W, Zhu J (2009) Carbon-coated silicon nanowire array films for high-performance lithium-ion battery anodes. *Appl Phys Lett* 95:133119.
15. Cao FF, et al. (2011) Cu-Si nanocable arrays as high-rate anode materials for lithium-ion batteries. *Adv Mater* 23:4415–4420.
16. Gogotsi Y, Simon P (2011) True performance metrics in electrochemical energy storage. *Science* 334:917–918.
17. Magasinski A, et al. (2010) High-performance lithium-ion anodes using a hierarchical bottom-up approach. *Nat Mater* 9:353–358.
18. Kasavajjula U, Wang C, Appleby AJ (2007) Nano- and bulk-silicon-based insertion anodes for lithium-ion secondary cell. *J Power Sources* 163:1003–1039.
19. Misra S, et al. (2012) In situ x-ray diffraction studies of (de)lithiation mechanism in silicon nanowire anodes. *ACS Nano* 6:5465–5473.
20. Huang Z, Geyer N, Werner P, de Boor J, Gosele U (2010) Metal-assisted chemical etching of silicon: A review. *Adv Mater* 23:285–308.
21. Kim J, Rhu H, Lee W (2011) A continuous process for Si nanowires with prescribed lengths. *J Mater Chem* 21:15889–15894.
22. Singh N, et al. (2012) Paintable Battery. *Sci Rep* 2:481, 10.1038/srep00481.
23. Barraclough KG *Waste Not, Want Not!—A Case for Recycling Silicon Waste Powder Kerf, KGBConsulting Ltd study*, http://www.kgbconsultingltd.com/.
24. Hochbaum AI, Yang P (2010) Semiconductor nanowires for energy conversion. *Chem Rev* 110:527–546.
25. Liu X, Long YZ, Liao L, Duan X, Fan Z (2012) Large-scale integration of semiconductor nanowires for high-performance flexible electronics. *ACS Nano* 6:1888–1900.
26. Weisse JM, Lee CH, Kim DR, Zheng X (2012) Fabrication of flexible and vertical silicon nanowire electronics. *Nano Lett* 12:3339–3343.
27. Caillon-Caravanier M, Claude-Montigny B, Lemordant D, Bosser G (2002) Absorption ability and kinetics of a liquid electrolyte in PVDF–HFP copolymer containing or not SiO_2. *J Power Sources* 107:125–132.
28. Sethuraman VA, Kowolik K, Srinivasan V (2011) Increased cycling efficiency and rate capability of copper-coated silicon anodes in lithium-ion batteries. *J Power Sources* 196:393–398.
29. Chen H, Xiao Y, Wang L, Yang Y (2011) Silicon nanowires coated with copper layer as anode materials for lithium-ion batteries. *J Power Sources* 196:6657–6662.
30. Memarzadeh EL, et al. (2012) Silicon nanowire core aluminum shell coaxial nanocomposites for lithium ion battery anodes grown with and without a TiN interlayer. *J Mater Chem* 22:6655–6668.
31. Kim J, Ryu J, Lee K, Oh S (2005) Improvement of silicon powder negative electrodes by copper electroless deposition for lithium secondary batteries. *J Power Sources* 147:227–233.
32. Usui H, Uchida N, Sakaguchi H (2011) Influence of order in stepwise electroless deposition on anode properties of thick-film electrodes consisting of Si particles coated with Ni and Cu. *J Power Sources* 196:10244–10248.
33. Murugesan S, Harris JT, Korgel BA, Stevenson KJ (2012) Copper-coated amorphous silicon particles as an anode material for lithium-ion batteries. *Chem Mater* 24:1306–1315.
34. Chen H, Xiao Y, Wang L, Yang Y (2011) Silicon nanowires coated with copper layer as anodes materials for lithium-ion batteries. *J Power Sources* 196:6657–6662.
35. Zhang H, Braun PV (2012) Three-dimensional metal scaffold supported bicontinuous silicon battery anodes. *Nano Lett* 12:2778–2783.
36. Zhang LQ, et al. (2011) Controlling the lithiation-induced strain and charging rate in nanowire electrodes by coating. *ACS Nano* 5:4800–4809.
37. Moshtev R, Johnson B (2000) State of the art of commercial Li ion batteries. *J Power Sources* 91:86–91.